J. Fluid Mech. (1965), *vol.* 21, *part* 2, *pp.* 241–255
Printed in Great Britain

Investigation of the flow behind a two-dimensional model with a blunt trailing edge and fitted with splitter plates

By P. W. BEARMAN
Engineering Laboratory, University of Cambridge

(Received 15 January 1964 and in revised form 19 June 1964)

The flow in the wake of a two-dimensional model with a blunt trailing edge was examined at Reynolds numbers (based on model chord) between $1{\cdot}4 \times 10^5$ and $2{\cdot}56 \times 10^5$. The ratio of total boundary-layer thickness at the trailing edge to model base height was approximately 0·5. Measurements were taken of base pressure and vortex shedding frequency together with traverses of the wake using a hot-wire anemometer. Traverses carried out along the wake showed a peak in the root-mean-square velocity-fluctuation at a distance equal to one base height from the model rear face. The position of the peak is referred to as the position of the fully formed vortex. The investigation was extended to a model fitted with splitter plates up to four base heights long. For each plate tested, a position of the fully formed vortex was found, and its distance from the model base was discovered to be inversely proportional to the base pressure coefficient. The flow about the model with splitter plates is described as being separated into five régimes of flow.

1. Introduction

A review paper by Nash (1962) emphasized the sparseness of existing knowledge about base flow at low speeds. Particular attention was drawn to the need for information on bluff bodies with small thickness-chord ratios. Some important work was carried out by Fage & Johansen (1927*a*, *b*) on the flow behind flat plates and various other shapes using an early form of hot-wire equipment. This type of approach has been employed by various later authors, including Kovasznay (1949), Roshko (1953) and Schaefer & Eskinazi (1959), for flow behind circular cylinders at very low Reynolds numbers. Little work has been carried out in the Reynolds number range considered here (from $1{\cdot}4 \times 10^5$ to $2{\cdot}56 \times 10^5$, based on model chord).

The free shear layers separating from a bluff body roll up to form vortices, and these vortices are shed alternately from each side of the body. It has long been known that splitter plates reduce the drag of a bluff body and in some cases suppress vortex formation. This investigation was carried out in order to examine more fully the phenomenon of vortex formation and the influence splitter plates have on the flow behind bluff bodies.

2. Experimental arrangement

The experiments were performed in a closed-return wind-tunnel having a working section 28 in. × 32 in. The tunnel speed ranged from 0 to 80 ft./sec giving Reynolds number R, based on model chord, up to $2{\cdot}56 \times 10^5$. Velocity fluctuations in the area occupied by the model and its associated wake were found to be everywhere less than 0·2 % of the local mean velocity at all speeds.

The bluff model used had a 28 in. span, 6 in. chord and a base height h of 1 in. The model cross-section consisted of a half ellipse with semi-major and -minor axes of 5 in. and 0·5 in. The rear 1 in. of the model was parallel-sided in order that the flow left the surface smoothly at the trailing edge corners. Transition wires were attached at 20 % chord. The boundary-layer thickness at the trailing edge was approximately 0·25 in. over the range of R investigated giving the ratio of total boundary-layer thickness to h as 0·5.

A row of pressure tappings was inserted across the base of the model to investigate the extent of three-dimensionality along the span. At mid-span, six tappings were placed across the base height to measure the pressure distribution and to obtain a representative value of base pressure. Full-span splitter-plates $\frac{1}{16}$ in. thick could be attached perpendicular to the rear face of the model at mid-base height. Splitter plates examined were within the range 0 to $4h$ long. The flow in the model wake was investigated using a DISA constant-temperature anemometer having a platinum-plated-tungsten wire of diameter 0·005 and length 1 mm. The hot wire could be traversed at the centre of the model span, along the wake (x, measured from the base), and perpendicular to the wake (y, measured from the wake centre line, positive upwards).

3. Discussion of experimental procedure and results

The experimental work can be separated into three parts: measurement of base pressure, measurement of shedding frequency, and hot-wire traverses.

3.1. *Measurement of base pressure*

The first case to be examined was for the model without a splitter plate. The spanwise distribution of base pressure is shown as the upper solid line in figure 1. It can be seen that there were considerable three-dimensional effects. The base pressure was much higher at the ends of the span, where high pressure air from the tunnel wall boundary layers flowed into the separated region of low pressure behind the model. Thus, in order to reduce this inflow, it was decided to attach end-plates at 1·5 in. from either wall. The boundary layer on these plates was much thinner than that on the tunnel walls, and consequently the inflow was reduced; the effectiveness of the end-plates is demonstrated in figure 1.

Figure 2 shows the pressure distribution across the base at mid-span. The base pressure coefficient $(C_p)_b$ was constant across the base height. It is interesting to note that fitting end-plates decreased base pressure by 1 or 2 %; therefore end effects must have reached to the centre of the model span. From figure 2, the value of $(C_p)_b$ at $y/h = 0$ was taken as the representative value of the model base pressure.

Splitter plates were then fitted, and the previous pressure measurements repeated for each plate length. Figure 3 shows a plot of $-(C_p)_b$ against splitter-plate length l divided by h. This graph has many interesting features, notably

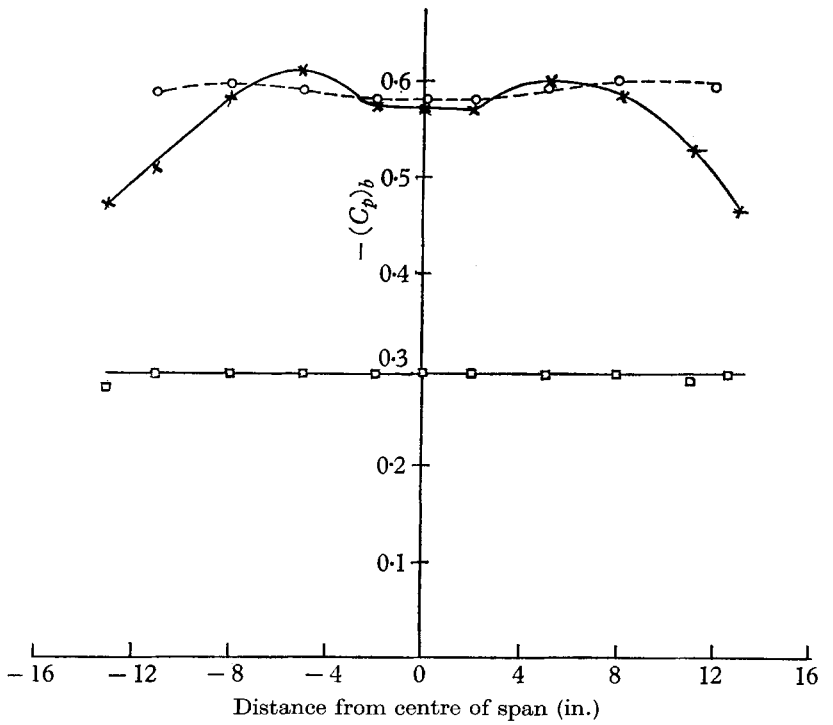

FIGURE 1. Spanwise base-pressure distribution. ×, without splitter plate and end-plates; ○, without splitter plate but with end-plates; □, with splitter plate of length $l/h = 1{\cdot}75$ but without end-plates.

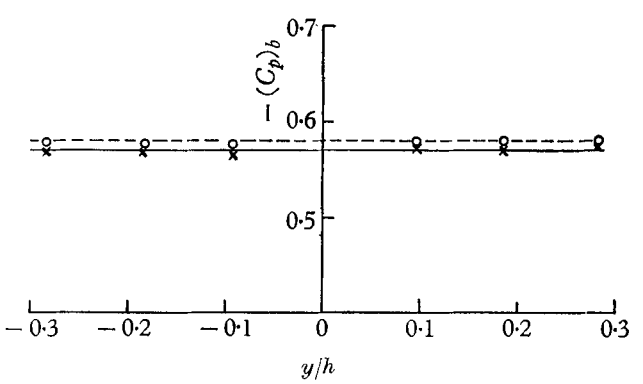

FIGURE 2. Base-pressure distribution across the base at mid-span without a splitter plate. ×, without end-plates; ○, with end-plates.

the sharp increase of base pressure (reduction of drag) for splitter-plate lengths up to $l/h = 1$. Beyond $l/h = 1$, $-(C_p)_b$ rises to a maximum at $l/h = 1{\cdot}5$, falling to a sensibly constant value of about 0·22 beyond $l/h = 2{\cdot}5$. Graphs of base pressure against splitter-plate length, for flow about a blunt base, have been

produced by Nash, Quincey & Callinan (1963) and show similar features to the above. Roshko (1954) has published a plot of the base pressure on a circular cylinder with a splitter plate of fixed length placed at various positions in the wake. A straight line has been drawn through the results whereas, if a curve is drawn connecting all the points, a graph similar to figure 3 is produced.

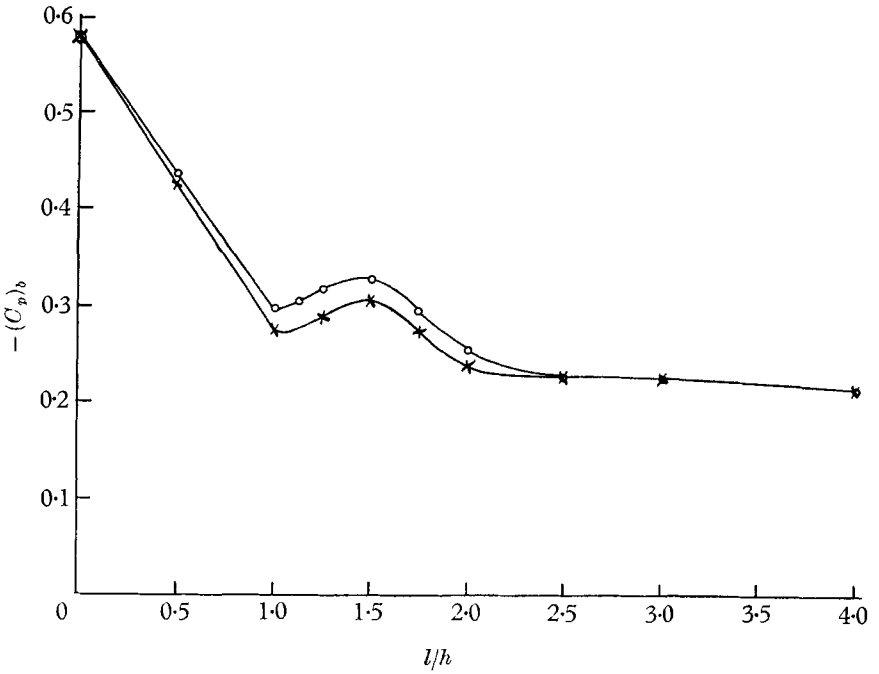

FIGURE 3. Base-pressure coefficient versus splitter-plate length.
×, $R = 1{\cdot}4 \times 10^5$; ○, $R = 2{\cdot}45 \times 10^5$.

Figure 3 shows a Reynolds number dependence, especially for splitter plates between $l/h = 1$ and 2. Beyond splitter-plate lengths of $2{\cdot}5h$, the base pressure appeared independent of R, which suggests that some steadier régime of flow had been established. It is proposed to discuss figure 3 in more detail later in conjunction with results obtained with the hot wire.

During the experiments providing figure 3, a number of interesting incidental observations were made. Beyond splitter-plate lengths of $1{\cdot}5h$, it was found that end-plates produced little improvement in the two-dimensionality of the flow; accordingly, they were removed to increase the effective span. The pressure distribution for a $1{\cdot}75h$ splitter plate without end-plates is shown in figure 1 and can be seen to be remarkably uniform across the span. For splitter plates greater than $l/h = 1$, a differential pressure was observed between the upper and lower surfaces of the plate if it was not exactly perpendicular to the rear face of the model. This effect became most marked at $l/h = 1{\cdot}5$. Although the base pressure distribution was changed, the overall base drag was found to remain constant.

To investigate the flow on the splitter plate, it was decided to use the surface oil film technique. The mixture used was one part of titanium dioxide and one part of linseed oil to five parts of 'Easy Nut' penetrating oil. Figure 4, plate 1,

shows a photograph, taken through the roof of the tunnel, of the oil-flow pattern on a splitter plate of length $4h$. Reattachment occurs at $2{\cdot}9h$ from the model trailing edge, and a secondary separation occurs at $x/h = 1{\cdot}15$. There is evidence of a secondary vortex flow very close to the rear face of the model. A small accumulation of oil is visible along the trailing edge of the plate, which is thought to have been caused by surface-tension effects around the end of the plate and not by flow separation. Figure 4 is consistent with photographs by Tani *et al.* (1961) of the flow over a step, aluminium powder in water being used to visualize the flow.

Oil-flow patterns for a splitter plate of length $3h$ showed a similar reattachment almost on the end of the plate at $2{\cdot}9h$. For $2{\cdot}0$ and $1{\cdot}5h$ plates, however, reattachment did not occur, but the secondary separation seemed unchanged, still taking place at $x/h = 1{\cdot}15$.

3.2. *Measurement of shedding frequency*

The next phase of the investigation consisted of an examination of the vortex-shedding frequency f of the model with splitter plates. An oscilloscope displaying the fluctuating voltage of a hot wire gives an accurate picture of the velocity fluctuations at the hot-wire probe. The optimum position of the wire, in order to obtain f, was first found by trial and error. Two general rules, however, were evolved: first, the wire should be placed just outside the wake, and secondly, the best streamwise position was downstream of the splitter plate but not more than one base height beyond the end. The hot wire was so arranged that it was mainly sensitive to velocity fluctuations in the main flow direction. The trace formed was virtually a sine wave of constant frequency and almost constant amplitude. A cycle represented the passage of one vortex from the vortex row springing from the corner of the model nearest the wire. From photographs showing a large number of cycles, it was a simple matter to extract a value of f. Figure 5 shows a typical plot of Strouhal number $S = fh/U_0$, where U_0 is free stream velocity, against R. It can be seen that there was a slight increase of S with R.

Strouhal number is plotted against l/h in figure 6 for $R = 1{\cdot}45 \times 10^5$ and $2{\cdot}45 \times 10^5$. This graph shows a maximum value of S between $l/h = 1{\cdot}25$ and $1{\cdot}5$. A Reynolds number effect was apparent for each splitter plate tested. It seems reasonable to suggest that this effect is associated with the similar effect found for base pressure in figure 3. Shedding was found to cease for a splitter plate of length somewhere between $2{\cdot}0$ and $2{\cdot}5h$. It was expected, from consideration of the oil-flow patterns, that no shedding would occur for splitter plates longer than $3{\cdot}0h$. No shedding at $l/h = 2{\cdot}5$ was, however, unexpected since it was known that reattachment occurred at $2{\cdot}9h$ from the base with a $3{\cdot}0h$ splitter plate. The base pressure recorded was identical to that for a plate with reattachment (see figure 3). If the flow reattached on the end of the $2{\cdot}5h$ splitter plate, a lower base pressure compared with $l = 3{\cdot}0h$ would be expected in order to curve the separation streamline round to attach at $2{\cdot}5h$ instead of $2{\cdot}9h$. One has to postulate, therefore, the flow forming a closed bubble beyond the end of the plate.

At a late stage in the investigation, a frequency analyser became available, and it was decided to use it to check the values of f found by the photographic method and also to examine more thoroughly the case when $l/h = 2{\cdot}5$. The output from

the analyser, which was plotted on an X-Y recorder, was proportional to the amplitude of velocity fluctuations at the hot wire. A typical plot is shown in figure 7 for a splitter plate of length $1{\cdot}5h$ at $R = 1{\cdot}4 \times 10^5$. To obtain this plot, the

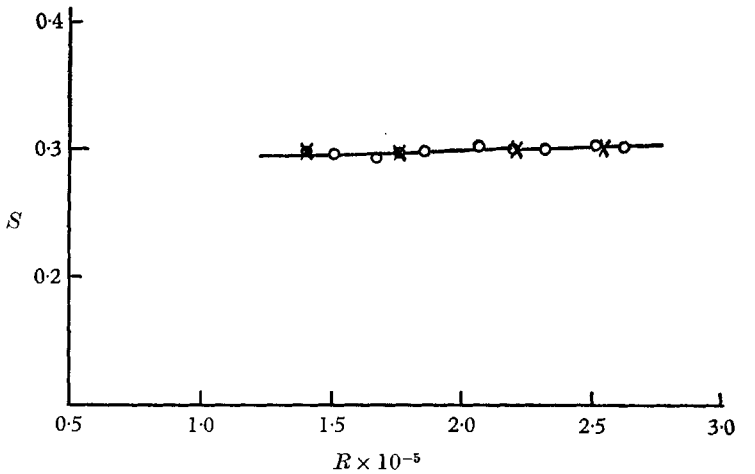

FIGURE 5. Strouhal number versus Reynolds number for a splitter plate of length $l/h = 1{\cdot}75$. ×, oscilloscope results; ○, frequency analyser results.

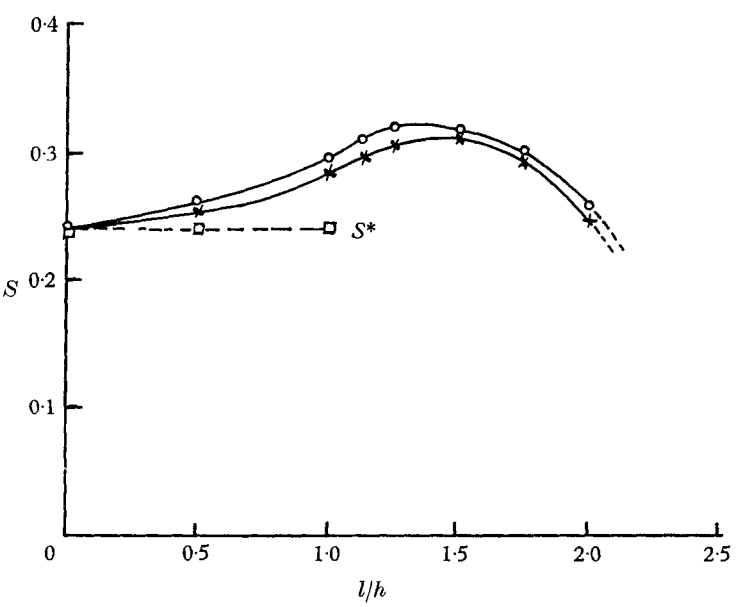

FIGURE 6. Strouhal number versus splitter-plate length. ×, $R = 1{\cdot}45 \times 10^5$; ○, $R = 2{\cdot}45 \times 10^5$; □, S^* at $R = 1{\cdot}45 \times 10^5$.

wire was placed just outside the wake where there was a very sharp peak produced by the velocity fluctuations at the shedding frequency. The very high degree of agreement found between the values of S obtained from the oscilloscope photographs and from the analyser is shown in figure 5.

Also visible in figure 7 is a very much smaller peak centred on twice the shedding frequency. This was caused by the velocity fluctuations produced by the vortex row on the opposite side of the wake which was 180° out of phase with the row on the nearside of the wake. In comparison with the magnitude of the velocity fluctuations at the shedding frequency, those at other frequencies were insignificant. This explains why the oscilloscope photographs of the hot-wire trace outside the wake gave such accurate values of f. At all positions across the

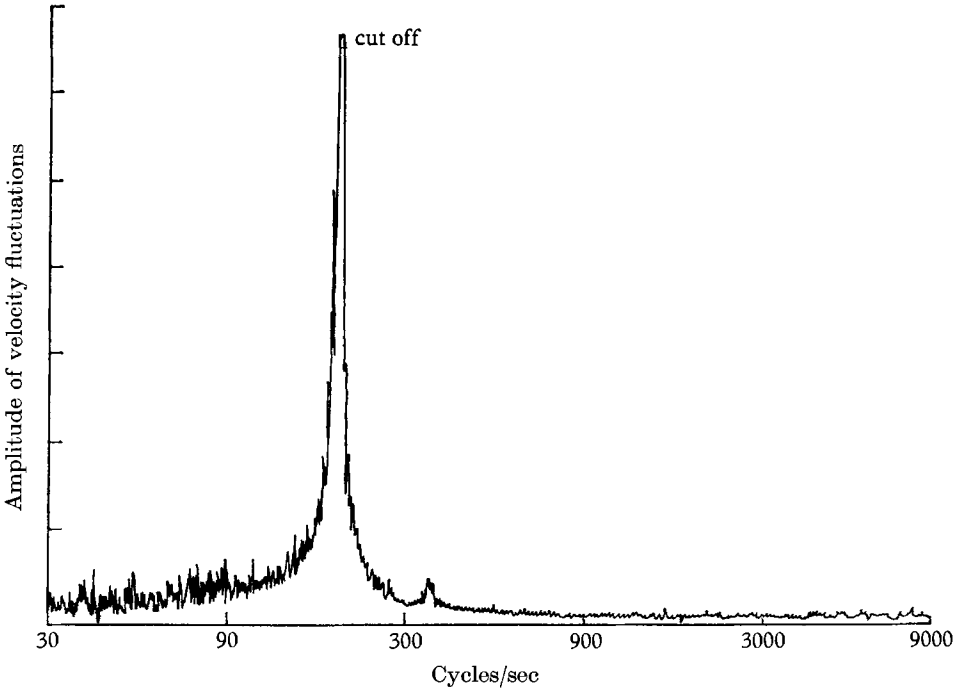

FIGURE 7. Amplitude of velocity fluctuations against frequency for a splitter plate of length $l/h = 1{\cdot}5$, at $R = 1{\cdot}4 \times 10^5$.

wake, the magnitude of velocity fluctuations associated with vortex shedding were found to be many times greater than those caused by general turbulence.

The main purpose of using the frequency analyser was to determine whether any characteristic frequency could be observed in the wake of the $2{\cdot}5h$ splitter plate. Many frequency traverses were performed inside and outside the wake but no predominant frequency could be found. It is interesting to note that figure 3 shows no sudden increase of base pressure when shedding stopped—somewhere between $l/h = 2{\cdot}0$ and $2{\cdot}5$.

3.3. *Results of hot-wire traverses*

The third stage of the investigation was a detailed examination of the model wake using a constant-temperature hot-wire anemometer. The hot wire measured the R.M.S. value of velocity fluctuations $u_{\text{R.M.S.}}$ and the mean flow velocity U at the wire. $u_{\text{R.M.S.}}$ is a measure of the velocity fluctuations in the streamwise direction

and the percentage velocity-fluctuation is often defined as $(u_{\text{R.M.S.}}/U) \times 100$. It was thought more useful, however, to base the percentage velocity-fluctuation measurements on the free stream velocity U_0. Basing the percentage velocity-fluctuations on U would give very high values near the model base, not necessarily because $u_{\text{R.M.S.}}$ was high, but because U was low. Thus for comparing velocity fluctuations at various positions behind the model it was decided to define the percentage R.M.S.-velocity-fluctuation θ as $(u_{\text{R.M.S.}}/U_0) \times 100$.

The first hot-wire traverse performed was along the x-axis of the wake ($y/h = 0$) for the model without a splitter plate (figure 8(*a*)). This plot showed a maximum value of θ at a distance of one base height behind the model. It seems reasonable to suggest that this peak has its origin in vortices which form from the rolling up of the free shear layers behind the body. It is proposed to call the position at which the velocity-fluctuation peak occurred the position of the fully formed vortex.

In order to interpret this hot-wire traverse more fully, it was decided to use a smoke tunnel where hot-wire traverses could be performed and photographs taken of the flow. The model used was of similar shape to the basic model but the maximum R that could be obtained was $0{\cdot}7 \times 10^5$ which produced laminar free shear layers downstream of the model. From a large number of photographs, mean positions were found for the first and second vortices of the street. The majority of photographs showed the first vortex in a stage of development. The corresponding hot-wire traverse exhibited the same features as that shown in figure 8(*a*). On the photographs, the θ peak occurred downstream of the first vortex but upstream of the second. It is suggested that it is within this region that one would expect to observe the fully formed vortex.

Returning to figure 8(*a*), it is seen that even in the so-called 'dead air' region just behind the model the velocity fluctuation recorded was very high. Very close to the body, where mean velocities were small, the hot wire may no longer have a linear response to small velocity fluctuations, and the values of θ obtained may only give a qualitative assessment of the velocity fluctuations there. In the region of vortex formation, however, the hot-wire recorded mean velocities of $0{\cdot}6$ to $0{\cdot}8U_0$. The velocity fluctuation peak decayed rapidly at first, but downstream of a position $2{\cdot}5h$ the rate of decay was fairly small.

Also plotted in figure 8(*a*) is the velocity fluctuation traverse at $y/h = 0{\cdot}25$. This was performed in order to find out if the same peak could be detected away from the wake centre line. Splitter plates were to be fitted to this basic model, and thus traverses would no longer be possible at $y/h = 0$, but it was hoped that the same technique could be used to detect vortex formation. Figure 8(*a*) shows that the velocity fluctuation peak appeared sharper but that it was still centred on $x/h = 1{\cdot}0$.

Further traverses were made for the basic model across the wake in the y-direction. These traverses are shown in figure 9, where only one half has been plotted since they were symmetrical about the wake centre line. Near the base, the traverses were characterized by very sharp peaks produced by passing through the turbulent free shear layers springing from the corners of the model. This peak moved in towards the centre of the wake and formed a maximum at

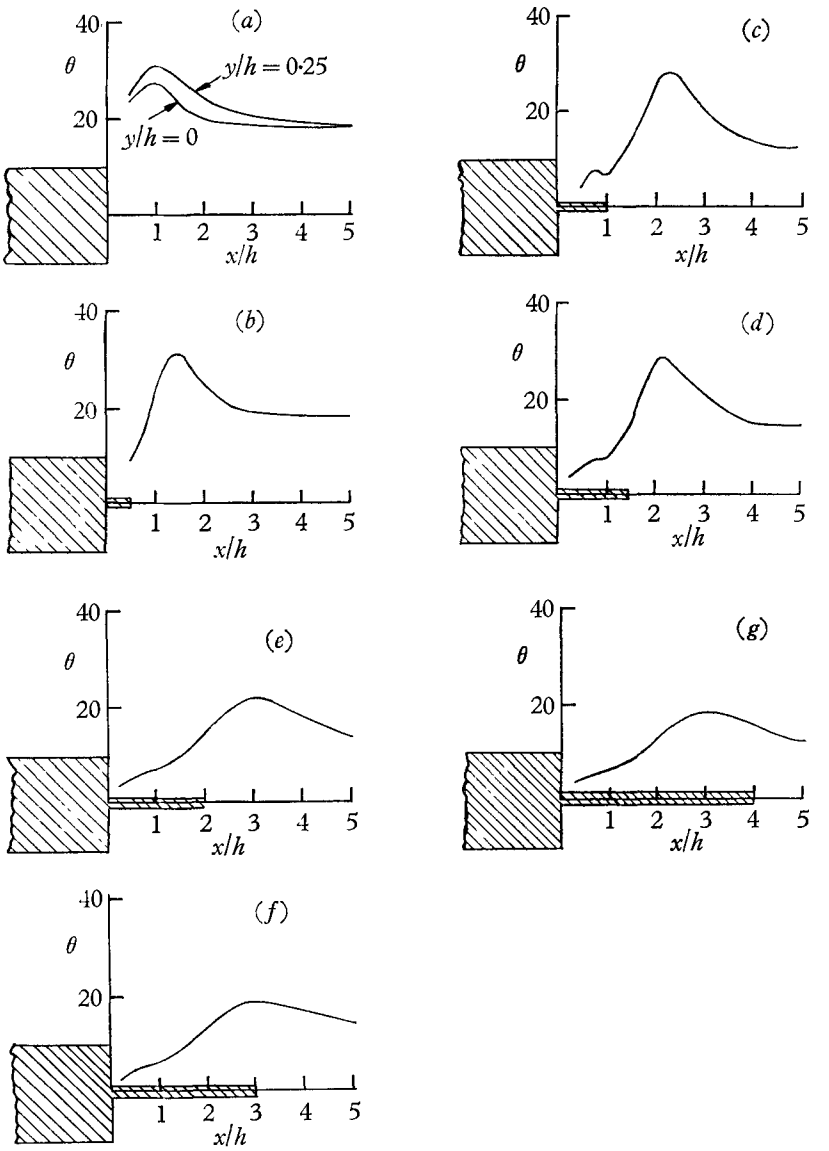

FIGURE 8. Percentage velocity-fluctuation traverses along the wake at $y/h = 0{\cdot}25$ for various splitter-plate lengths at $R = 1{\cdot}4 \times 10^5$. (*a*) $l/h = 0$, (*b*) $l/h = 0{\cdot}5$, (*c*) $l/h = 1{\cdot}0$, (*d*) $l/h = 1{\cdot}5$, (*e*) $l/h = 2{\cdot}0$, (*f*) $l/h = 3{\cdot}0$, (*g*) $l/h = 4{\cdot}0$.

a distance of one base height. The peak then moved outwards from the centre line and weakened in intensity.

Many authors including Kovasznay (1949), Roshko (1953) and Schaefer & Eskinazi (1959), examining the wakes of circular cylinders at low R, have stated that positions of maximum velocity fluctuation are coincident (or in the case of Schaefer & Eskinazi, nearly coincident) with positions of vortex centres. Schaefer & Eskinazi point out that the maximum velocity fluctuation occurs in

the immediate vicinity of the vortex-core edge farthest from the street centre-line. Traverses carried out behind the model in this investigation (although at a much higher R and with turbulent boundary layers on the model) show similar features to those found by the above authors. To a first approximation at least, it can be said that downstream of vortex formation, positions of maximum θ, taken from traverses across the wake, give the lateral spacing of the vortices. To show this more clearly, the positions of maximum θ are plotted in figure 10 (*a*). Also shown on this graph is the position of maximum θ (position of the fully formed vortex) taken from streamwise traverse at $y/h = 0{\cdot}25$ (figure 8 (*a*)).

As already stated there was a convergence of the velocity-fluctuation peaks to the position of maximum velocity fluctuation (one base height) and then a divergence. This necking effect was found by Schaefer & Eskinazi (1959) again for the flow behind circular cylinders at low R. They state that at each R the distance at which the minimum spacing of the paths of vortex centres occurred

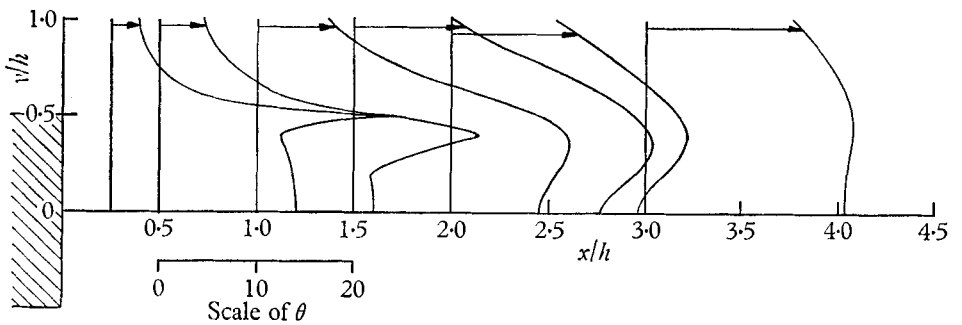

FIGURE 9. Percentage velocity-fluctuation traverses across the wake without a splitter plate, $R = 1{\cdot}45 \times 10^5$.

was nearly coincident with the position of maximum velocity fluctuation. They define this position as the start of the fully developed street. The region between the cylinder producing the vortices and the point of minimum spread of vortices is referred to as the formation region.

Having developed a method for examining the vortex street, it was now decided to extend the investigation to the basic model fitted with splitter plates. Figure 8 is a plot of θ traverses along the wake at $y/h = 0{\cdot}25$ for selected splitter-plate lengths. The most interesting feature of these plots is the downstream displacement of the peak in θ suggesting that vortices are being formed further from the model base. Compared with the model without a splitter plate (figure 8 (*a*)), the values of θ were much less within the region close behind the model. With splitter-plate lengths $l/h = 0{\cdot}5$ to $1{\cdot}0$, large increases of θ did not occur until beyond the end of the plate. For splitter plates having $l/h > 1{\cdot}0$, the rise began before the end of the plate indicating a different régime of flow with vortices commencing to form in the shear layers above and below the splitter plate. It is evident from figure 3 that a fundamental change in flow régime occurred for $l/h > 1{\cdot}0$ with $-(C_p)_b$ increasing with increasing l/h. It is thought that this effect was due to the fact that vortices could no longer be persuaded to form beyond the end of the splitter plate. Nash *et al.* (1963) have suggested the

existence of two flow régimes, one appropriate to short, and a second to long splitter plates.

Some recent experiments have shown that when the hot-wire signal was filtered, allowing only fluctuations at the vortex-shedding frequency to pass, the distribution of θ was similar to that for the unfiltered signal. For splitter plates

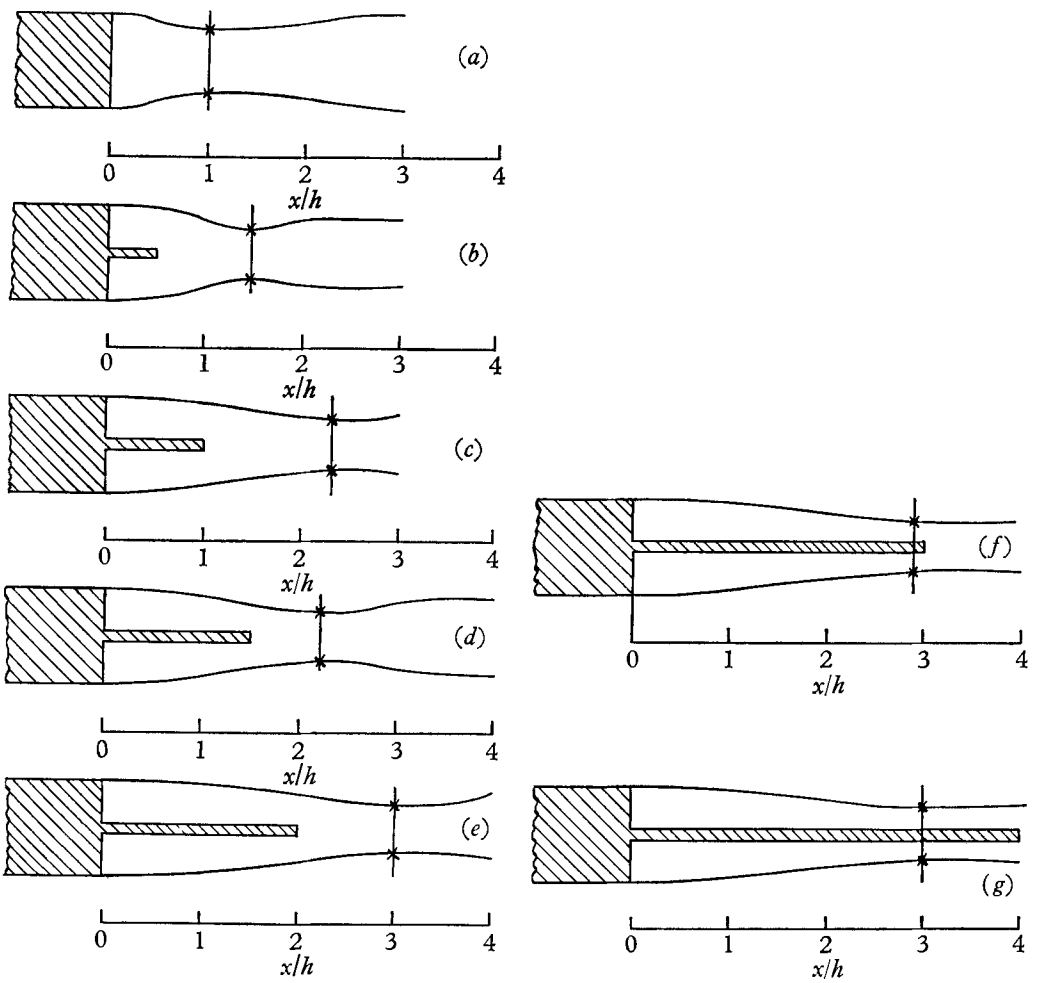

FIGURE 10. Plots of positions of maximum θ taken from traverses across the wake for various splitter-plate lengths at $R = 1{\cdot}45 \times 10^5$. ×, position of maximum θ taken from streamwise traverse at $y/h = 0{\cdot}25$. (*a*) $l/h = 0$, (*b*) $l/h = 0{\cdot}5$, (*c*) $l/h = 1{\cdot}0$, (*d*) $l/h = 1{\cdot}5$, (*e*) $l/h = 2{\cdot}0$, (*f*) $l/h = 3{\cdot}0$, (*g*) $l/h = 4{\cdot}0$.

up to $l/h = 2{\cdot}0$, the peak value of θ still occurred at about the same streamwise position. Thus in the shedding cases (figures 8(*a*) to (*e*)), the θ peak was representative of the fluctuations associated with vortex shedding.

As stated earlier, it appeared that, for $l/h > 3{\cdot}0$, the stable situation of flow over a step had been established. The velocity-fluctuation traverses for $l/h = 3{\cdot}0$ and $4{\cdot}0$ are shown in figures 8(*f*) and (*g*). It is interesting to note that a maximum

value of θ occurred above the position of flow reattachment as obtained by the oil-film technique. This is in agreement with Tani, Jucki & Komoda (1961) who observed that, in the reattachment region of flow over a step, θ reached a maximum value.

In order to investigate more fully the various flow régimes, a number of hot-wire traverses across the wake were carried out in a similar manner to those shown in figure 9. The positions of the maximum values of θ taken from these plots are shown in figures 10(*b*) to (*g*). As in figure 10(*a*), the peak velocity-fluctuation points converged to the point of maximum velocity fluctuation and

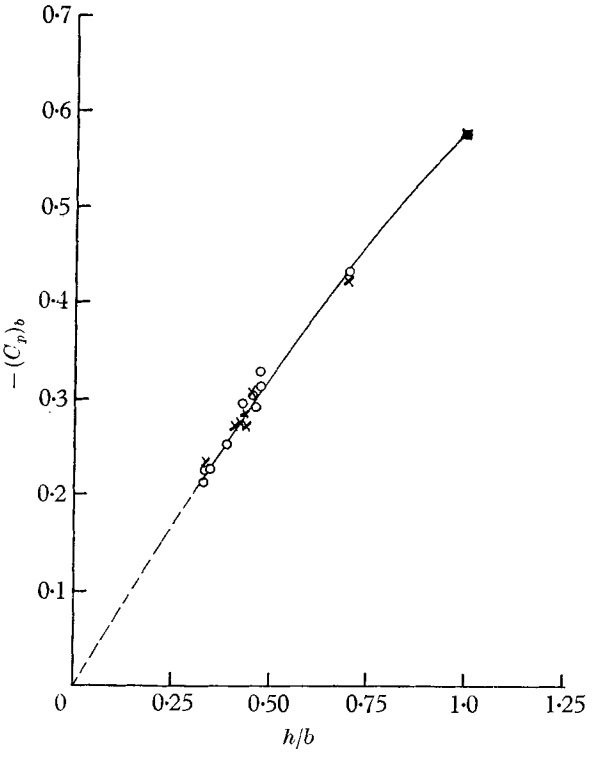

FIGURE 11. Base-pressure coefficient against inverse of vortex formation position. ×, $R = 1{\cdot}45 \times 10^5$; ○, $R = 2{\cdot}25 \times 10^5$.

then diverged. For all splitter plates examined, the absolute maximum value of θ occurred at the throat, where the distance between peaks was approximately $0{\cdot}5h$. Figure 10 confirmed that traverses along the streamwise direction were best performed at $y/h = 0{\cdot}25$. Performing traverses between $y/h = 0{\cdot}25$ and $0{\cdot}5$ would produce twin peaks, and traversing at $y/h < 0{\cdot}25$ would give a less sharp peak.

It appears evident from figure 8 that, since splitter plates force vortex formation downstream, the base pressure will be dependent on the distance b of the peak in θ from the base of the model. $-(C_p)_b$ is plotted against h/b in figure 11, which shows that the base pressure was approximately inversely proportional

to the distance to the position of the fully formed vortex. This graph is plotted for the two Reynolds numbers $1{\cdot}45 \times 10^5$ and $2{\cdot}25 \times 10^5$ and shows a collapse of the data. At the lower R, the vortices formed further from the body, and the base pressure $-(C_p)_b$ was correspondingly lower.

The curve in figure 11 appears to pass through the origin which suggests that if b could go to infinity $(C_p)_b$ would approach zero. The results obtained when there was no vortex shedding also lie on the curve. With flow reattachment, b was equal to the distance to the reattachment point. For the condition without shedding and without reattachment ($l/h = 2{\cdot}5$), the maximum value of θ occurred above the proposed free stagnation point.

4. Régimes of flow

The flow over the model with splitter plates can best be summarized by separating it into a number of different régimes.

4.1. *Régime* 1—*splitter plates* $l/h = 0$–$1{\cdot}0$

The basic model produced vortices at a distance downstream equal to one base height, and the effect of a splitter plate was to push vortex formation a further splitter-plate length downstream. Thus for a splitter-plate length $l/h = 0{\cdot}5$, vortices appeared fully formed at a distance of about $1{\cdot}5h$. In this régime, base pressure was proportional to splitter-plate length. The splitter plate effectively increased the chord of the model, and vortices began to form from an imaginary base in the plane of the end of the splitter plate.

There was a large pressure difference across the shear layers and they curved in towards the splitter plate (figure 10(*b*) and (*c*)). Thus, the actual wake thickness at the start of vortex formation was smaller than for the basic model. Fage & Johansen (1927*b*) suggested a wake Strouhal-number $S^* = fd/U_0$ which was a function of wake thickness d. Stouhal number, as plotted in figures 5 and 6, is normally defined as

$$S = fh/U_0.$$

Therefore

$$S = S^*h/d.$$

A representative value of wake thickness d can be obtained if it is assumed that the distance between peaks of θ at the end of a splitter plate is equal to the distance between the free shear layers. Klebanoff (1954) showed that in a turbulent boundary layer the maximum value of θ occurred very close to the surface. Thus in the case without a splitter plate, where vortices began to form immediately behind the body, $d = h$, giving $Sd/h = 0{\cdot}24 = S^*$. Values of Sd/h, for splitter plates $l/h = 0$ to $1{\cdot}0$, are plotted in figure 6 and give the constant value of $0{\cdot}24$ at $R = 1{\cdot}45 \times 10^5$.

4.2. *Régime* 2—*splitter plates* $l/h = 1{\cdot}0$–$1{\cdot}5$

It is reasonable to suppose that a free shear layer can only be extended a certain length before it breaks down into vortices. This limit appeared to be one base height because there is evidence to show that, for splitter-plate lengths of more

than $1{\cdot}0h$, the shear layers began to break down upstream of the end of the splitter plate. Fully formed vortices were not developed, however, until they were well clear of the end of the plate. Base pressure coefficient $-(C_p)_b$ increased during this régime, and, on the assumption of the position of the fully formed vortex being inversely proportional to base pressure, the position of this vortex must move closer to the base. This was observed by the hot wire (figure 10 (*c*) and (*d*)). The Strouhal number reached a maximum of 0·32 at l/h between 1·3 and 1·5, and $-(C_p)_b$ reached a maximum between $l/h = 1{\cdot}4$ and 1·5.

Photographs of the flow behind blunt trailing edge bodies, fitted with splitter plates (e.g. Thomann 1959 and Nash *et al.* 1963) clearly indicate the difference between régimes 1 and 2.

4.3. *Régime* 3—*splitter plates* $l/h = 1{\cdot}5$–$2{\cdot}0$ *approximately*

In this régime $-(C_p)_b$ and S decreased. The position of the fully formed vortex once more moved downstream, as in régime 1, thus decreasing $-(C_p)_b$. In traverses of the hot wire in the streamwise direction, comparatively high values of θ were recorded towards the end of the splitter plate (figure 8 (*e*)). Hot-wire records showed a more gradual rise to the peak of maximum velocity fluctuation followed by a more gradual decay.

4.4. *Régime* 4—*splitter plates* $l/h = 2{\cdot}0$–$3{\cdot}0$ *approximately*

In this régime the flow exhibited no pronounced shedding frequency. The only experimental value in this régime is for a splitter plate of length $2{\cdot}5h$. Oil-flow patterns displayed no reattachment on the plate although the base pressure recorded was identical to that obtained with longer plates when reattachment did occur. This régime will be discussed further after régime 5.

4.5. *Régime* 5—*splitter plates* $l/h = 3{\cdot}0$ *approximately* $-\infty$

In régime 5 there was no vortex shedding, suggesting that the flow had reattached to the plate, and the oil-flow patterns showed a reattachment line at $2{\cdot}9h$. The base pressure coefficient, $-0{\cdot}22$, was the same as that found in régime 4 and is in agreement with results by Nash *et al.* (1963) for flow over a rearward-facing step.

Returning to régime 4, if the flow reattached on the end of the splitter plate, a lower base pressure (compared with régime 5) would be expected. Oil-flow patterns gave no indication of reattachment. One is left with the idea of a closed bubble with a free stagnation point at about 2·9 base heights downstream of the base. Hot-wire traverses behind the model at $y/h = 0{\cdot}25$ showed a peak of θ at $x/h = 2{\cdot}9$ which is consistent with the idea of the free shear layers coming together at this point. In this régime, there was insufficient plate length to produce reattachment and insufficient interaction between upper and lower shear layers to cause shedding.

The author gratefully acknowledges the suggestions of Dr D. J. Maull who has supervised this research. The author was in receipt of a grant from the Department of Scientific and Industrial Research.

REFERENCES

FAGE, A. & JOHANSEN, F. C. 1927*a* *Aero. Res. Coun., Lond., R. & M.*, no. 1104.
FAGE, A. & JOHANSEN, F. C. 1927*b* *Aero. Res. Coun., Lond., R. & M.*, no. 1143.
KLEBANOFF, P. S. 1954 *Nat. Adv. Comm. Aero., Wash., Tech. Note*, no. 3178.
KOVASZNAY, L. S. G. 1949 *Proc. Roy. Soc.* A, **198**, 174–90.
NASH, J. F. 1962 *Aero. Res. Coun., Lond., R & M*, no. 3323.
NASH, J. F., QUINCEY, V. G. & CALLINAN, J. 1963 *Aero. Res. Coun., Lond., Rep.* no. 25,070.
ROSHKO, A. 1953 *Nat. Adv. Comm. Aero., Wash., Tech. Note*, no. 2913.
ROSHKO, A. 1954 *Nat. Adv. Comm. Aero., Wash., Tech. Note*, no. 3169.
SCHAEFER, J. W. & ESKINAZI, S. 1959 *J. Fluid Mech.* **6**, 241–60.
TANI, I., JUCHI, M. & KOMODA, H. 1961 *Aero. Res. Inst. Univ. of Tokyo, Rep.* no. 364.
THOMANN, H. 1959 *F.F.A. Rep.* no. 84.